VERTICAL MOTION FIELD IN THE MIDDLE THERMOSPHERE FROM SATELLITE DRAG DENSITIES

R. E. DICKINSON and J. E. GEISLER*

Massachusetts Institute of Technology, Cambridge, Mass.

ABSTRACT

The vertical motion field in the thermosphere is calculated from the continuity equation. This calculation is based on a field of horizontal winds and an intermediate model of the thermospheric temperature field consistent with the density structure inferred from satellite drag data. The vertical motion consists of a component due to rise and fall of constant pressure surfaces and a component due to horizontal mass divergences, both components being of the order of 1 m. sec.$^{-1}$ Only the latter component is of importance for thermodynamic considerations. The adiabatic warming associated with the diurnally variable part of the vertical motion due to mass divergence gives a *second heat source* which is of magnitude comparable to the heating by solar radiation. The time-averaged meridional circulation also implies large adiabatic warming and cooling. This computed mean meridional circulation cannot be reconciled with the heat balance of the thermosphere. The thermospheric temperature field at low levels in high latitudes can be changed so as to reverse the direction of the mean meridional pressure gradient and thus to give a mean meridional circulation consistent with heat balance considerations. Existing global thermospheric models could be improved by adjustment of the temperature field at low levels in such a way that vertical motions computed from horizontal winds give a plausible adiabatic heating field.

1. INTRODUCTION

Atmospheric densities above 200 km. are deduced from the drag that the atmosphere exerts on artificial earth satellites. Various investigators (Harris and Priester [5]; Jacchia [7]; Jacchia and Slowey [8]) have made use of the densities to formulate models describing the temperature and density structure of the thermosphere above the 120-km. level. The dominant time-variable component is a diurnal thermal tide, referred to as the *diurnal bulge*. From the temperature field of the models referenced above one can deduce pressure gradients and hence the forcing of motions. Horizontal winds have been derived in this way assuming a balance of pressure gradient forces with combined inertial, ion drag, and viscous drag forces (Geisler [4]; Kohl and King [10]; Lindzen [13]). Direct wind measurements (King-Hele and Allen [9]) give little information on the horizontal variation of motions. One purpose of this paper is to present and describe the field of *vertical* velocity calculated from the horizontal wind system of Geisler [4]).

It has been established by a scale analysis of the relevant equations (Dickinson, Lagos, and Newell [2]; Lagos [11]) that vertical motions in the thermosphere have an amplitude of the order of 1 m. sec.$^{-1}$ Adiabatic heating by such motions is of the same magnitude as the solar heating by extreme ultraviolet radiation. The integration of a two-dimensional numerical model of the thermosphere, coupling the equations of motion and the thermodynamic equation, was described in these papers. The numerical model showed maximum heating by vertical motions occurring late in the morning, shifting the phase of the diurnal bulge to a time 3 hr. earlier than that given by a one-dimensional diffusion model. The second purpose of this paper is to use the vertical velocities calculated from the horizontal winds of Geisler [4] to investigate further the adiabatic heating by vertical motions. This horizontal wind system was calculated from a given model of the thermospheric temperature and density fields (Jacchia and Slowey [8]) which is based on satellite drag data in both high and low latitudes. Certain features of the latitudinal distribution of adiabatic heating deduced from these winds are found to be unacceptable from a thermodynamic standpoint. The third purpose of the paper is to suggest changes in the given thermospheric temperature model which can produce an acceptable adiabatic heating pattern without rendering the model inconsistent with the satellite drag data.

2. BACKGROUND AND THEORETICAL FORMULATION

Some basic features of the global model of the thermosphere (Jacchia and Slowey [8], hereafter referred to as JS) and details of the horizontal wind system derived from it (Geisler [4], hereafter referred to as Paper I) are briefly reviewed in this section. Following this review, we sketch the derivation of two well-known equations of fluid dynamics in a form suitable for application to diurnal tidal motions in the thermosphere. These equations are the continuity equation, by means of which we deduce vertical motions from the horizontal winds of Paper I; and the thermodynamic equation, from which we obtain the heating implied by these vertical motions.

THE HORIZONTAL WIND SYSTEM

The global model of JS is based on theoretical density profiles calculated by integrating the hydrostatic equation

*Present affiliation: University of Miami, Coral Gables, Fla.

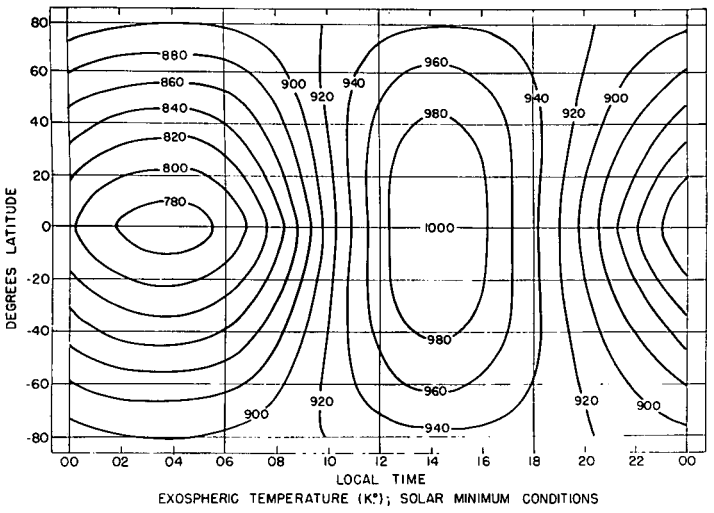

FIGURE 1.—The exospheric temperature field for the JS model used in Paper I. Temperatures in °K.

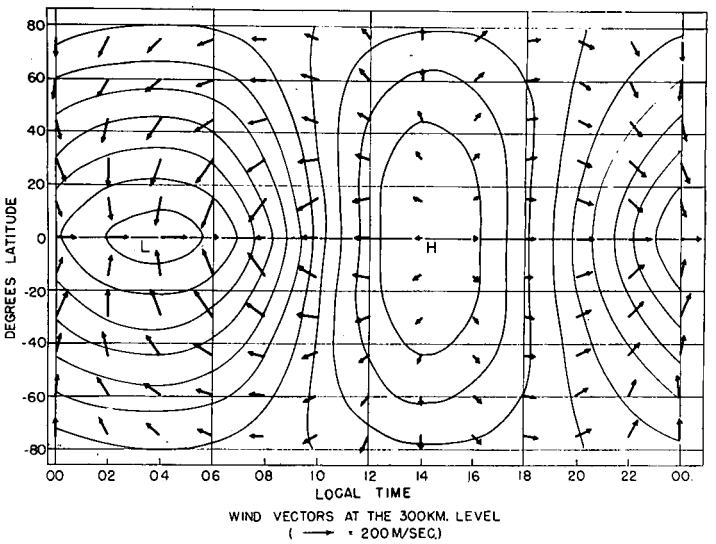

FIGURE 2.—The horizontal wind pattern at 300 km. from Paper I shown against a background of isobars at this level. The longest arrow represents a wind speed of 225 m. sec.$^{-1}$

upward from the 120 km. level for each atmospheric constituent. The temperature is assumed to vary with altitude z above this level according to the relation

$$T=T_\infty+(T_0-T_\infty)\exp[-sz]. \tag{1}$$

In this equation T_0 is the temperature at the 120-km. level and s is a parameter governing the shape of the profile. The temperature approaches at great heights the limiting value T_∞, referred to as the *exospheric temperature*. This temperature model was apparently first introduced by Bates [1]. Treating the exospheric temperature as a function of latitude and local time, JS determined a global pattern of exospheric temperature which reproduced the density pattern inferred from the available satellite drag data. The pattern of exospheric temperature from which the pressure gradients employed in Paper I were calculated is shown in figure 1. In this and other figures to follow, the abscissa may be regarded either as local time or as longitude (in units of hours) at a fixed time.

In Paper I, horizontal winds were computed over the globe at closely spaced intervals in the vertical between 140 km. and 500 km. A cross section at the 300-km. level is shown in figure 2, arrows indicating the vector wind. As noted in that paper, isotherms of exospheric temperature are also isobars at all altitudes. In general, the horizontal velocity field is divergent in the vicinity of the maximum of the diurnal bulge and convergent in the vicinity of the minimum. A further feature which is evident in this figure is that the zonally averaged meridional wind is directed toward the Equator in all latitudes. The form of the wind pattern is similar at every level to that seen in figure 2. The vertical variation of the wind is discussed in Paper I.

INTEGRAL FORM OF THE CONTINUITY EQUATION

To obtain a form of the continuity equation from which vertical motions may be calculated, consider a column of unit horizontal area bounded from below by a constant pressure surface $p=p_0$ at a height $h=h(p_0)$ and extending to very great heights. Since the atmosphere up through the thermosphere occurs in a shell, thin compared to the radius of the earth, we may to a first approximation neglect the variation of gravity and of the spherical coordinate system metric with radial distance from the center of the earth. The pressure at a point is then proportional to the total atmospheric mass per unit horizontal area above the given point. Hence the total mass in the column above a constant pressure surface is conserved; that is, if $\mathcal{J}_S$ is the net inflow through the sides and $\mathcal{J}_B$ is the net inflow through the bottom of the column, then

$$\mathcal{J}_S+\mathcal{J}_B=0. \tag{2}$$

All vectors in the following argument will be in the horizontal plane. If we take ρ to be the mass of the atmosphere per unit volume and $\mathbf{c}$ to denote the horizontal velocity vector, the side inflow is clearly

$$\mathcal{J}_S=-\operatorname{div}\left[\int_{h(p0)}^{\infty}\rho\mathbf{c}\,dz\right].$$

The bottom inflow $\mathcal{J}_B$ is the sum of the mass flow through unit area of the p_0 surface by horizontal motions in amount $-\rho\,\mathbf{c}\cdot\nabla h$, and by vertical motions in amount $\rho(w-\partial h/\partial t)$. The quantity h denotes the height of a given constant pressure surface, $\partial h/\partial t$ is the vertical velocity of this surface, ∇h the angle this surface makes with the horizontal, and w the vertical velocity. Thus from (2), the vertical velocity at the pressure surface p_0 is given by

$$w=w_D+w_L, \tag{3}$$

where

$$w_D=\frac{1}{\rho(h)}\operatorname{div}\left[\int_{h(p0)}^{\infty}\rho\mathbf{c}\,dz\right], \tag{4}$$

$$w_L=\left(\frac{\partial h}{\partial t}+\mathbf{c}\cdot\nabla h\right)_{p=p_0} \tag{5}$$

It was shown by scale analysis (Dickinson et al. [2]) that $\partial h/\partial t>>\mathbf{c}\cdot\nabla h$ for planetary scale diurnal motions with velocities of the order of 100 m. sec.$^{-1}$ or less. Equation (3) then states that upward vertical motion on the surface $p=p_0$ is given by the sum of two terms: a) w_D, the vertical motion determined from the total mass divergence above h; b) $w_L\simeq\partial h/\partial t$, the vertical velocity given by lifting of the constant pressure surface.

To interpret further the w_D vertical velocity, we make use of the hydrostatic equation

$$\frac{\partial p}{\partial z}=-\rho g, \tag{6}$$

from which one obtains the relationship

$$\frac{Dp}{Dt}=\rho g\left[\left(\frac{\partial h}{\partial t}+\mathbf{c}\cdot\nabla h\right)_p-w\right],$$

where D/Dt is the substantial time derivative. This may be written, using equation (5), as

$$-\frac{1}{\rho g}\frac{Dp}{Dt}=w-w_L; \tag{7}$$

the velocity w_D determined by mass divergence is therefore proportional to the negative change of pressure following a parcel of fluid. It is seen from equation (7) that equation (4) is equivalent to the usual p-coordinate system continuity equation (see, for instance Hess [6], p. 262).

THE THERMODYNAMIC EQUATION

The thermodynamic equation, describing the change in time of temperature T, is written

$$c_p\frac{DT}{Dt}-\frac{1}{\rho}\frac{Dp}{Dt}=Q \tag{8}$$

where c_p is specific heat at constant pressure and Q is the rate of heat addition per unit mass. The heating Q is taken to describe all entropy-increasing processes, including heat conduction and heating by solar radiation. The substantial time derivative evaluated on a constant pressure surface may be written using equations (3) and (7) as

$$\frac{D}{Dt}=\left(\frac{\partial}{\partial t}+\mathbf{c}\cdot\nabla\right)_p+w_D\frac{\partial}{\partial z}.$$

The vertical motion w_L, resulting from lifting and falling of pressure surfaces, does not contribute to heating by motions.

The substantial derivative of temperature can be approximated by $\partial T/\partial t+w_D\partial T_m/\partial z$, where $T_m=T_m(z)$ is a mean temperature depending only on z (Dickinson, Lagos, and Newell [2]). It follows from this result and

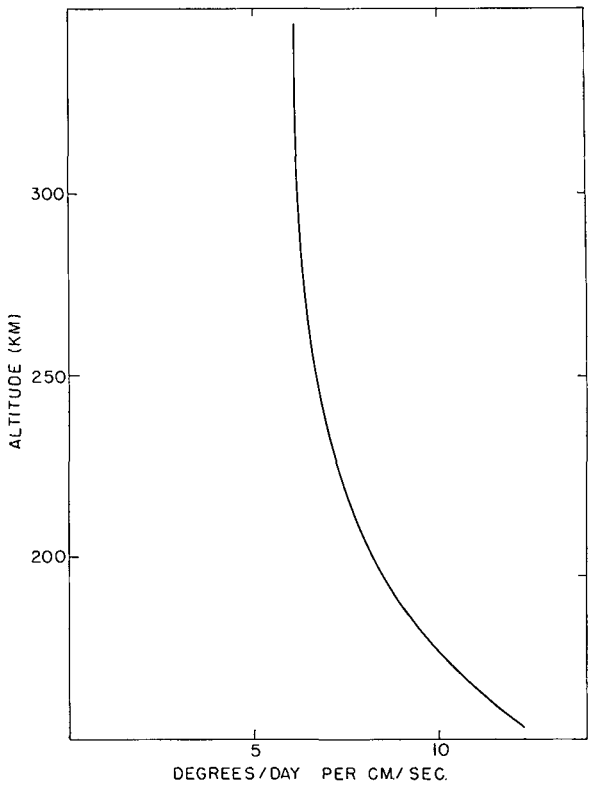

FIGURE 3.—The term $(\Gamma_a-\Gamma)=g/c_p+\partial T/\partial z$, the difference between adiabatic and model lapse rates as a function of altitude.

equation (7) that the thermodynamic equation may be written

$$\frac{\partial T}{\partial t}=\frac{Q}{c_p}+w_D(\Gamma-\Gamma_a) \tag{9}$$

where $\Gamma(z)=-\partial T_m/\partial z$ is the mean lapse rate and $\Gamma_a=g/c_p$ is the adiabatic lapse rate. The thermosphere is a stably stratified region, so that $\Gamma-\Gamma_a$ is negative. In figure 3 is shown $\Gamma_a-\Gamma$ when $T_m(z)$ is defined by the $T_\infty=900$°K. temperature profile used in Paper I. It may be seen from this figure that the heating per unit mass resulting from a vertical motion of 1 m. sec.$^{-1}$ decreases from about 1500°K. day^{-1} in the lower thermosphere to a limiting value of about 600°K. day^{-1} at great heights. Figure 4 (provided by C. P. Lagos and based on computations reported in Lagos and Mahoney [11]) shows the heating per unit mass by solar radiation at 30° lat. as a function of altitude and local time. Use will be made of these two figures in the following sections.

3. RESULTS AND DISCUSSION

THE CALCULATED VERTICAL MOTIONS

As discussed in section 2, the vertical velocity associated with diurnal thermospheric motions consists of the component w_D defined by mass divergence and the component w_L given by the rising and falling of constant pressure surfaces. The term $\partial h/\partial t\simeq w_L$ evaluated in the vicinity of the 300-km. level is presented in figure 5. This term has

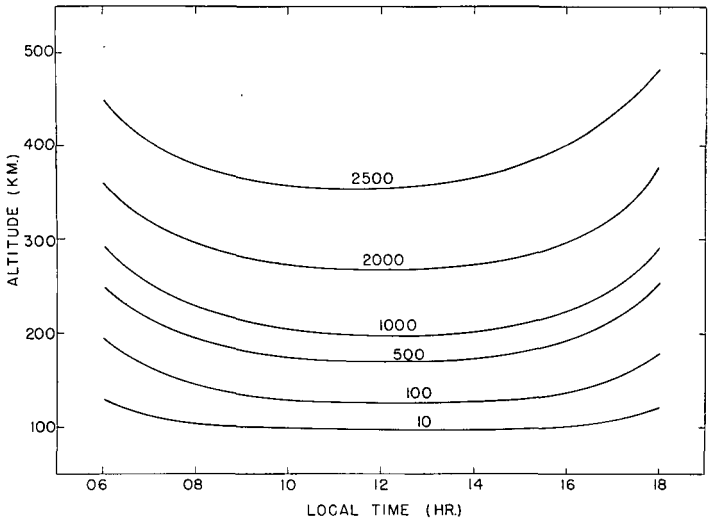

FIGURE 4.—Heating in degrees per day by solar radiation as a function of altitude and local time at 30° lat. and equinox.

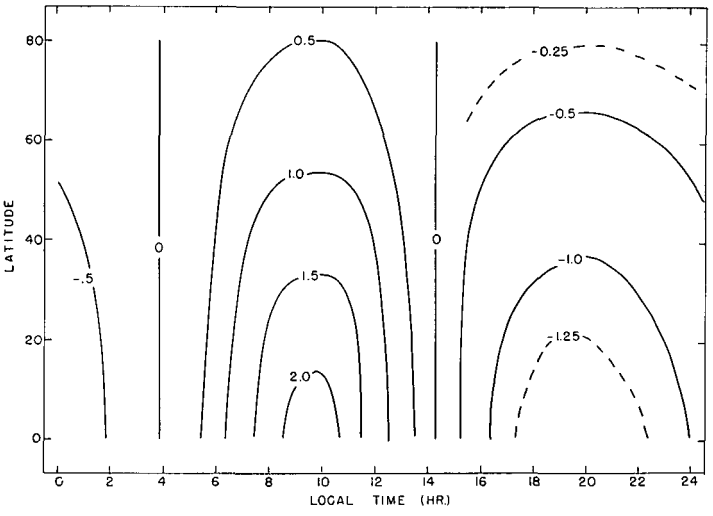

FIGURE 5.—The global field of vertical velocity $w_L=\partial h/\partial t$ at 300 km. arising from the lifting and falling of constant pressure surfaces. Units are m. sec.$^{-1}$

been calculated from the JS model for the exospheric temperature pattern shown in figure 1. Figure 5 shows an upward motion in the morning and a downward motion in the evening, consistent with the rise and fall of the diurnal bulge. This component of the vertical motion will not be discussed further, except to note that for time-periodic motions its average around a latitude circle will necessarily vanish.

The w_D vertical motion component may be written as the sum of the average around a latitude circle and the deviation from that average,

$$w_D=\overline{w}+w_D' \tag{10}$$

where

$$\overline{w}=(2\pi)^{-1}\int_0^{2\pi} w\,d\lambda$$

using λ as longitude. For discussion of the relation of the eddy vertical motion w_D' to horizontal winds, it is convenient to use the further decomposition

$$w_D'=w_D^{(z)}+w_D^{(m)} \tag{11}$$

where $w_D^{(z)}$ is the contribution to w_D' from the divergence of zonal (i.e. west to east) motion and $w_D^{(m)}$ is the contribution to w_D' from the divergence of meridional (south to north) motion. In the following discussion we shall refer to the respective terms in the decomposition defined by equation (11) as the *zonal wind vertical motion* and the *meridional wind vertical motion.*

TABLE 1.—*Zonal average of computed vertical motion at 300 km.*

Latitude	7.5	22.5	37.5	52.5	70
$\overline{w}$(m. sec.$^{-1}$)	−3.10	0.86	1.25	1.24	0.84

Values obtained for $\overline{w}$ at 300 km. are given in table 1. A broad pattern of mean rising motion is indicated over most latitudes with a zone of strong downward motion near the Equator. The same pattern persists down to the lower boundary at 140 km. The horizontal branch of this mean meridional circulation, as inferred from figure 2, consists of equatorward motions increasing as low latitudes are approached, to a maximum amplitude at around 15° of lat., then decreasing to zero at the Equator. This thermally indirect mean meridional circulation is considered highly unrealistic, as will be discussed further in section 4.

The eddy vertical motion is described by figures 6 through 9. Regions of downward vertical motion are shaded in these figures. Figures 6 and 7 show, respectively, the values at 300 km. of the zonal wind vertical motion and the meridional wind vertical motion. Both figures show in low latitudes an upward motion from 11 hr. to 22 hr., with maximum values near 16 hr. Both figures also show in low latitudes a downward motion pattern from 23 hr. to 10 hr. with a maximum around 6 hr.

Between latitudes of 20° and 40°, the phase of the meridional wind vertical motion changes rapidly. In latitudes above about 40°, the zonal wind and meridional wind vertical motion are out of phase by nearly ½ a day and their sum is reduced accordingly. In high latitudes the cancellation of the two terms is almost complete. Relatively large increments (15° of lat. and long.) were used in computing the horizontal wind divergences; truncation and plotting errors are expected to be of the same magnitude in polar latitudes as the sum of the two terms.

The phase shift of the meridional wind vertical motion from low to high latitudes occurs with a northwest-southeast tilt of the motion pattern. The downward zonal wind vertical motion pattern shows a smaller tilt in the same direction, the phase of maximum $w_D^{(z)}$ downward motion in figure 6 shifting from its value at the Equator to 00 hr. at high latitudes. The satellite drag data resolving the longitudinal density gradients (and hence exospheric temperature gradients) are much more extensive than those

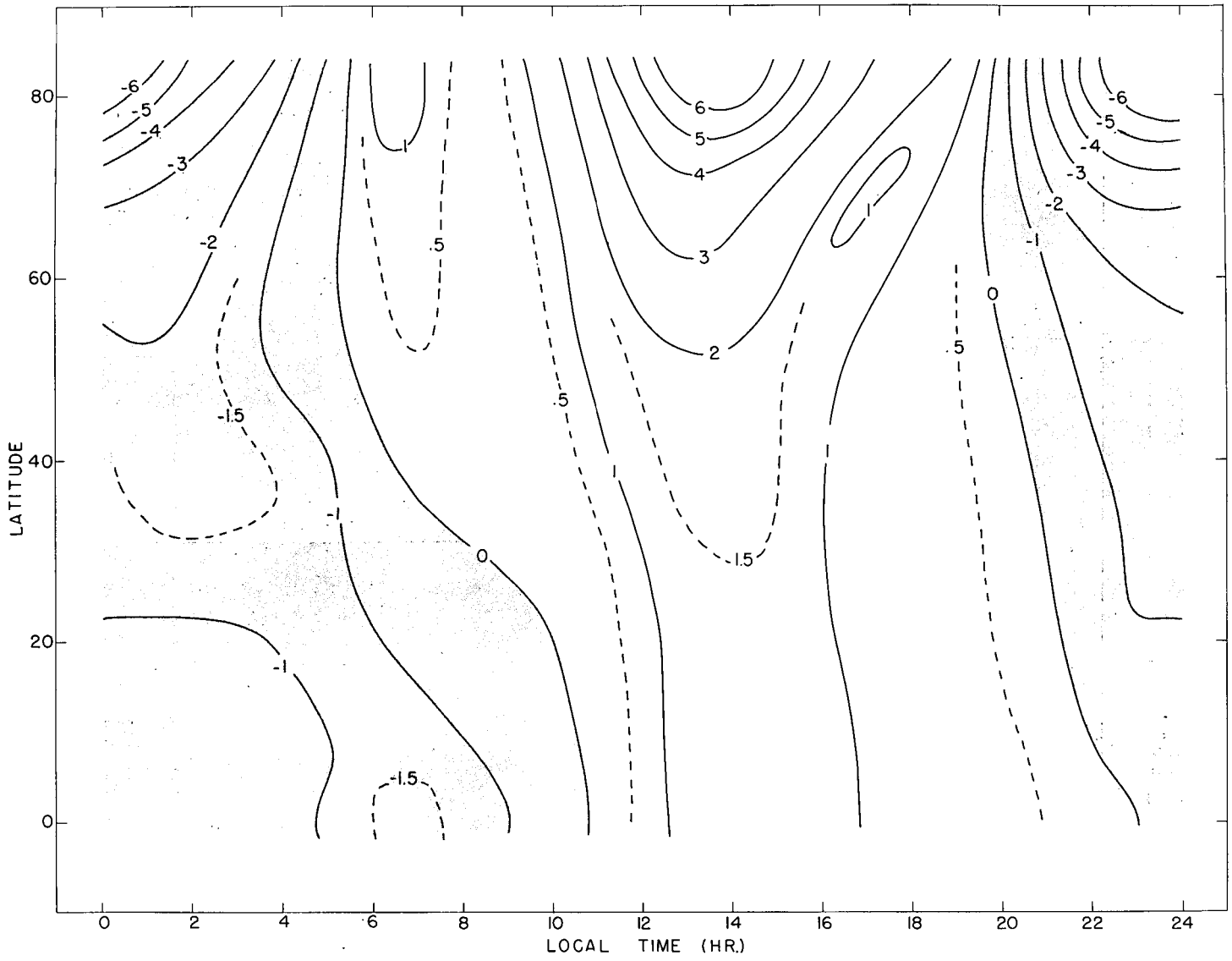

FIGURE 6.—The global field at 300 km. of the zonal wind vertical motion. Units are m. sec.$^{-1}$

resolving the latitudinal density gradients. For this reason, the zonal wind vertical motion pattern is considered to be more reliable than the meridional wind vertical motion pattern. For instance, it is not unreasonable to expect that there exists some other model consistent with density observations in which the nightside isotherms shown in figure 1 are pushed up into higher latitudes. The lines of zero vertical motion in figure 7 would then also be expected to be displaced poleward.

Figures 8 and 9 show longitude-altitude sections of the zonal wind and meridional wind vertical motion, respectively, at a lat. of 37.5°. The phase of these vertical motion terms remains essentially constant with altitude, but the amplitudes decrease by a factor of three in going from 300 km. to 150 km. A certain amount of distortion in the otherwise smooth patterns is seen to occur near sunrise at 06 hr. local time and near sunset at 18 hr. local time. This results from adjustment of the horizontal wind pattern during the changeover between the daytime and the nighttime ion concentration profiles, as described in Paper I.

DIURNAL HEATING PATTERN

The decomposition of the w_D field of vertical motion into a mean and an eddy term, as defined by equation (10), is useful in discussing separately the diurnally varying and mean components of heating due to vertical motions. That is, to a first approximation, we consider the zonal average and the deviation fields of temperature and density to be uncoupled. The pattern of heating due to the zonal average vertical motion will be discussed further in section 4.

The radiational drive of the diurnal bulge is effectively situated in the region between 150 and 250 km. where the heating rate per unit volume is maximum. The temperature at higher levels is maintained at nearly the temperature of the *drive region* by conduction. According to

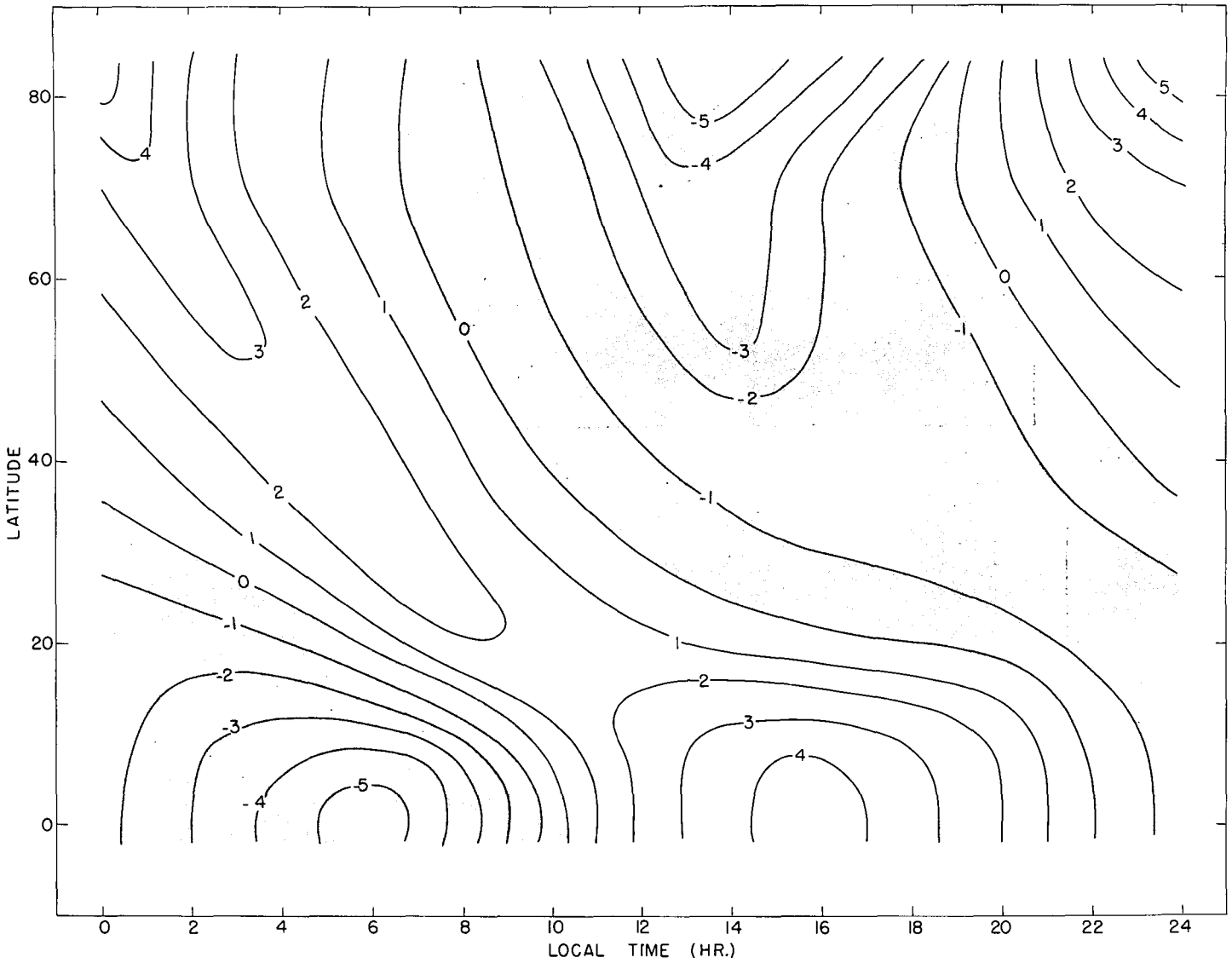

FIGURE 7.—The global field at 300 km. of the meridional wind vertical motion. Units are m. sec.$^{-1}$

figures 8 and 9, the vertical motion is roughly a factor of two less in the drive region than at the 300-km. level, and this is also true at other latitudes. The solar heating per unit mass, as indicated by figure 4, is also a factor of two less at 200 km. than at 300 km., but it decreases more rapidly than vertical motion amplitudes below this level. It follows that if we compare, at the 300-km. level, the adiabatic heating by vertical motions with the heating by solar radiation, we obtain a lower bound on the relative importance of adiabatic compared to solar heating in maintaining the diurnal bulge. The vertical velocities in figures 6 and 7 may be converted to heating rates through multiplication by the negative of the factor $(\Gamma_a - \Gamma)$, shown in figure 3.

The amplitude of the diurnal component of solar radiation is seen from figure 4 to be around 1000° per day at the 300-km. level. By comparison, figures 6 and 7 indicate that the diurnal component of the adiabatic heating rate amplitude is larger than 3000° per day at the 300-km. level in low latitudes. This result supports the conclusion of Dickinson, Lagos, and Newell [2] that adiabatic heating by vertical motions is fully as potent a heat source as solar radiation. Furthermore, the phase of the adiabatic heating pattern in low latitudes is such as to explain the observation that the diurnal bulge phase is 3 to 4 hr. earlier than that predicted by model calculations involving only solar heating. In these model calculations, cooling by downward conduction of heat does not check the upward expansion of the thermosphere until 17 or 18 hr. This time will be brought forward by the adiabatic cooling, which begins near 10 hr. and reaches a maximum near 16 hr.; and also by the adiabatic heating, which begins near 21 hr. and reaches a maximum around 6 hr.

If the zonal wind vertical motion is considered alone, the adiabatic heating and cooling in middle latitudes also act to advance the phase of the diurnal bulge. However, comparison of figures 8 and 9 reveals that the net adiabatic cooling at a lat. of 37.5° is much reduced during the

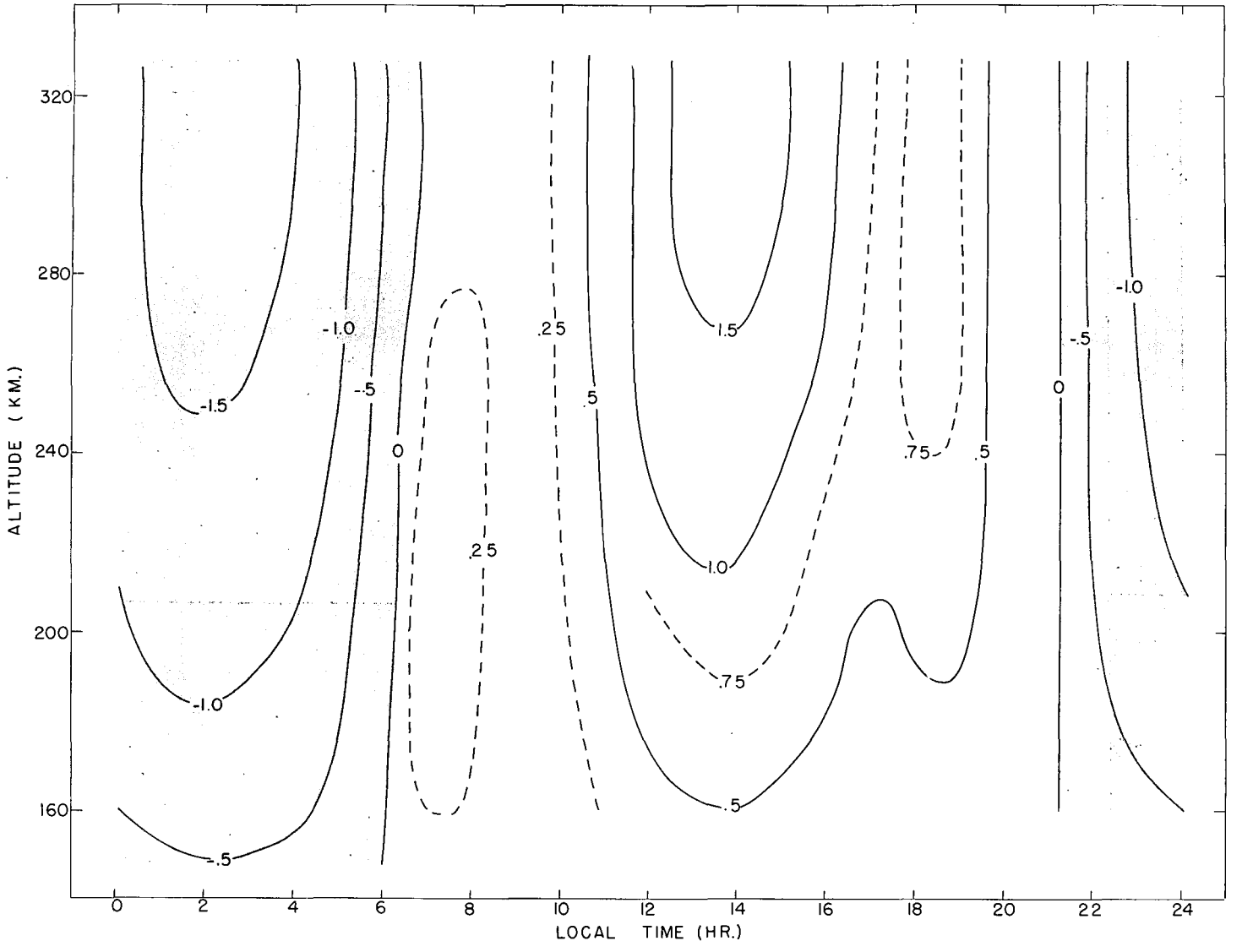

FIGURE 8.—A longitudinal section at 37.5° lat., showing the zonal wind vertical motion as a function of altitude in units of m. sec.$^{-1}$

afternoon and there is adiabatic *cooling* of significant amount in the predawn hours. Such a dramatic change in the distribution of adiabatic heating in local time between equatorial latitudes and a lat. of 37.5° is inconsistent with the latitudinal invariance of the phase of the diurnal bulge that is a built-in feature of the JS model. If this aspect of the JS model is correct, it appears that the phase reversal of the meridional wind vertical motion that occurs between low and high latitudes takes place at too low a latitude.

4. LATITUDINAL STRUCTURE AND THERMODYNAMIC CONSIDERATIONS

THE MEAN LATITUDINAL STRUCTURE OF THE MODEL

Let us consider now some features of the zonally averaged temperature field and pressure gradient field for the JS model used in Paper I. The temperature field is entirely specified by the exospheric temperature pattern, shown in figure 1, and by equation (1) with $T_0=355°K.$ and $s=0.028$ km.$^{-1}$ As described by Jacchia [7], the parameter s depends on exospheric temperature, but this variation of s is negligible over the range of exospheric temperatures in figure 1. For convenience of presentation, the zonally averaged temperatures have been subtracted from the reference temperature profile which is given by equation (1) with $T_\infty=900°K.$ The result shown in figure 10 indicates a temperature increase from Equator to Pole at all levels.

The zonally averaged pressure gradient force constructed on the basis of these temperatures is shown in figure 11. This force is directed from Pole to Equator at all levels and increases in amplitude until equatorial latitudes are reached, where it drops rapidly to zero. Such a pressure gradient force in the lower atmosphere would be expected to produce a vast anticyclonic circumpolar vortex, such as is found in the upper stratosphere in summer. In the thermosphere, where ion drag and molecular viscosity are large, the zonally averaged motion as deduced from this force is predominantly equatorward. The values of mean vertical velocities given in table 1 are upward in all latitudes except for a convergent region near the Equator.

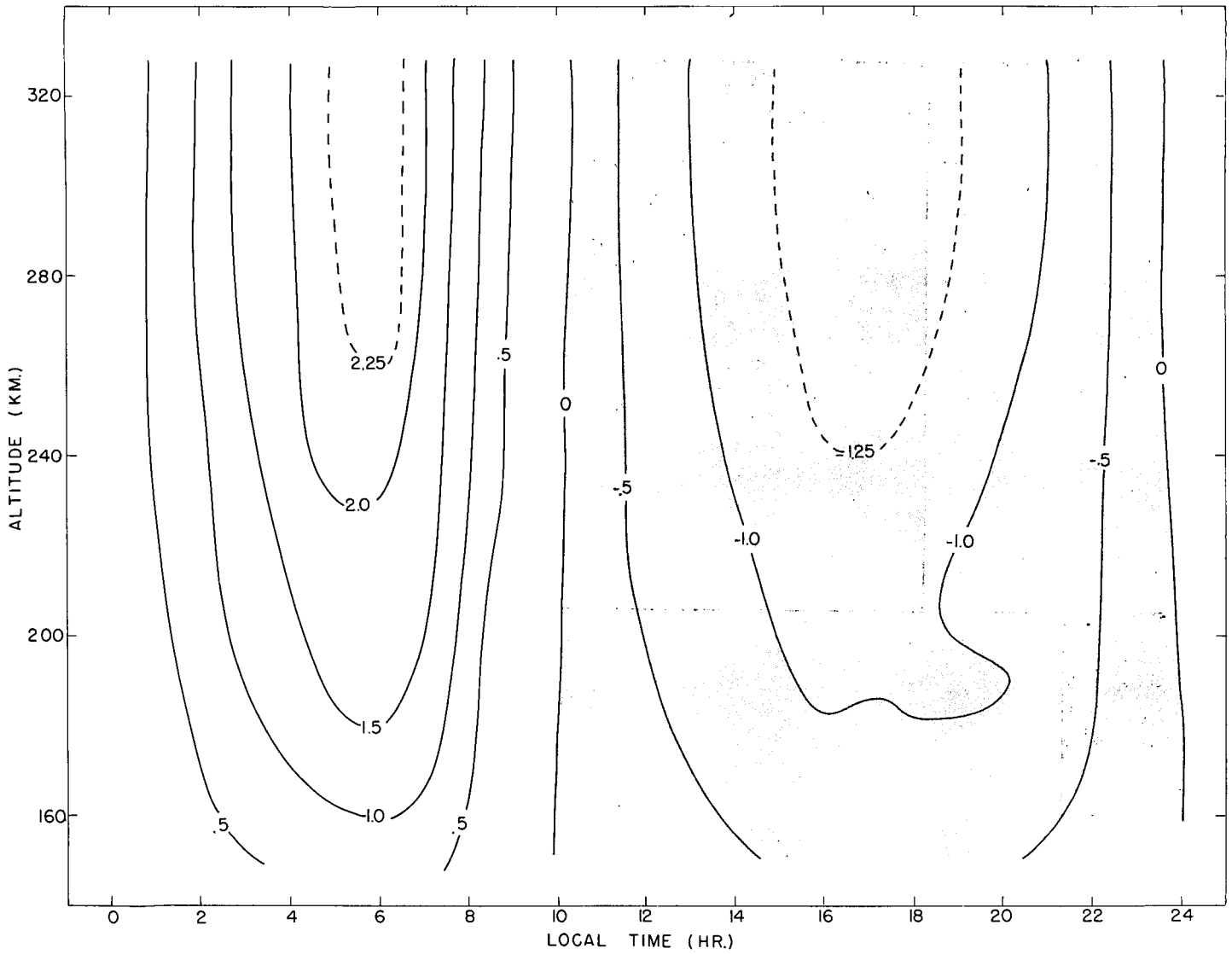

FIGURE 9.—A longitudinal section at 37.5° lat., showing the meridional wind vertical motion as a function of altitude in units of m. sec.$^{-1}$

The poleward increase of temperature shown in figure 10 is required to explain—within the framework of the JS model—the increase of density with latitude observed at high levels. This increase has been established by the analysis of the drag experienced by the polar-orbiting satellites Explorer XIX and Explorer XXIV, with perigees of 600 km. and 550 km., respectively. However, there are two physical objections to a poleward increase of temperature at all levels in the thermosphere. First, solar radiation would give maximum heating where it is coldest and minimum heating where it is warmest. Such a thermodynamic process is entirely incapable of maintaining the kinetic energy of winds at all levels against dissipation by ion drag and viscosity. It is thus essential from the viewpoint of thermospheric energetics that there be a mean poleward decrease of temperature at the lower levels of the thermosphere, where solar heating per unit volume is largest (Newell [14]). The second objection is that calculations by Lagos and Mahoney [12] of the maintenance of thermospheric temperatures by solar heating alone indicate that near the equinoxes high latitude temperatures are approximately ⅔ as large as equatorial temperatures, and at the winter solstice the high latitude temperatures are ⅓ of the equatorial values. They obtained densities at high levels near the Pole very much lower than near the Equator, except for a brief period near the summer solstice. Clearly some large, poleward-increasing heat source must be invoked to explain how temperatures increasing poleward, as in the JS model, could be maintained.

An attractive hypothesis for explaining the observed poleward increase of atmospheric density at high levels is that there be a meridional circulation of approximately the same intensity as that deduced from the winds of Paper I, *but oppositely directed.* In order to reverse the mean pressure gradient which drives the circulation, it is necessary to modify the temperature structure in the thermospheric model in such a way that the temperature decreases poleward in the relatively massive atmospheric layers below 200 km. With such a modification, the lower thermosphere will operate as a heat engine, maintaining

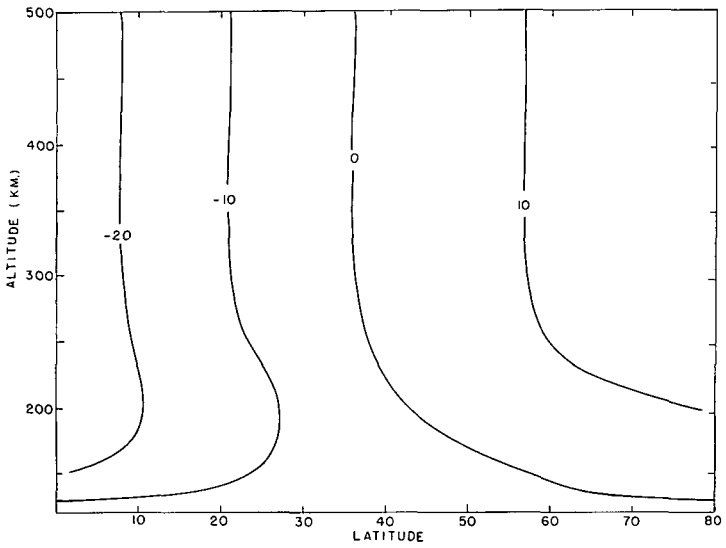

FIGURE 10.—The structure of the zonally averaged temperature field of the model used to compute pressure gradients in Paper I. Temperatures (in °K.) expressed as the deviation from a reference temperature.

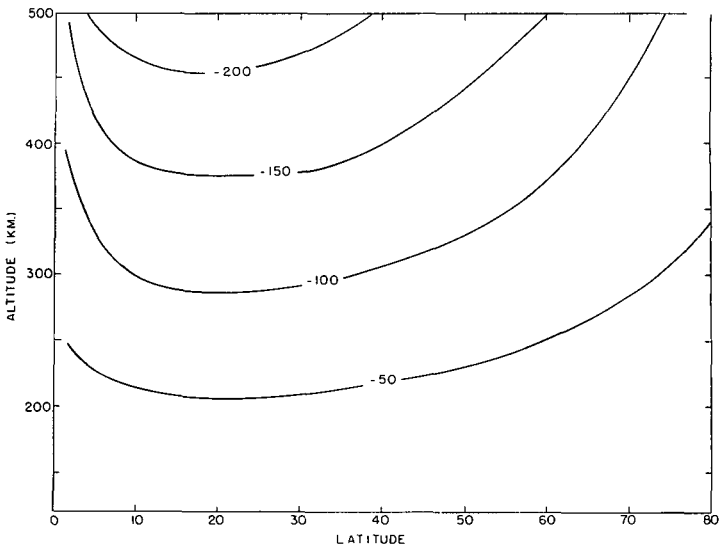

FIGURE 11.—The zonally averaged pressure gradient force obtained from the temperature field of the previous figure. Units are 10^{-4} m. sec.$^{-2}$

the kinetic energy of winds against dissipation; furthermore, subsidence in high latitudes will give additional heating there.

MODIFICATION OF THE MEAN LATITUDINAL STRUCTURE

One possible generalization of the JS model is to take s to vary with latitude. The parameter s determines the exponential decay away from the lower boundary of the difference between the exospheric temperature and the temperature at a given height. This decay rate is diminished by decrease of s, thereby decreasing also the temperature. The maximum temperature reduction occurs at the level $z=s^{-1}$.

Satellite drag data in high latitudes is presently available only at such great altitudes that these data provide essentially no direct information as to how the parameter s does in fact vary with latitude. We will assume here that one is free to vary s with latitude so as to generate energetically more satisfactory thermosphere models. (An alternative method of introducing the desired latitudinal variation of thermal structure would be to allow the parameter m of the JS model to vary with altitude, but this will not be considered here.) In the appendix is sketched an analysis of the dependence of pressure gradients on the two parameters T_∞ and s.

In order to illustrate the changes which take place when s is taken to decrease with latitude, we assume a simple variation of the form

$$s=s_0[1+b\ (\phi/90)^2]^{-1}. \qquad (12)$$

In this expression, ϕ is latitude in degrees, and b is a constant.

Temperature profiles have been calculated at successive latitudes from equation (1) using the variation of s given by equation (12) with $b=0.5$, $s_0=0.028$ km.$^{-1}$, and with the zonally averaged T_∞ for the pattern in figure 1. The zonally averaged temperature field thus obtained is

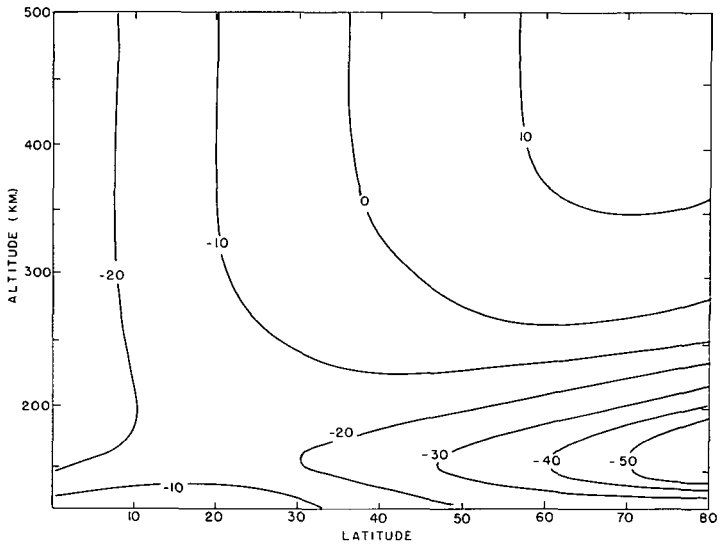

FIGURE 12.—The structure of the zonally averaged temperature field in the modified model. Units are the same as in figure 10.

illustrated in figure 12. Again the temperatures have been subtracted from the reference temperatures defined by the profile with $T_\infty=900$°K. and $s=s_0$. The temperature field in figure 12 is to be compared with that in figure 10. The sign of the temperature difference between low and high latitudes is now reversed below about 250 km.

The zonally averaged temperature field in figure 12 has been used to evaluate the parameters A and B defined in the appendix; zonally averaged meridional pressure gradients have been subsequently calculated from equation (A.3), assuming the dependence of s upon latitude given by equation (12) with $b=0.5$. This field of pressure gradient force is illustrated in figure 13. This is to be compared with the result obtained when s is independent of latitude as illustrated in figure 11. The pressure gradient force is now seen to be directed toward the Pole, except at high levels in the Tropics. The variation of the wind with

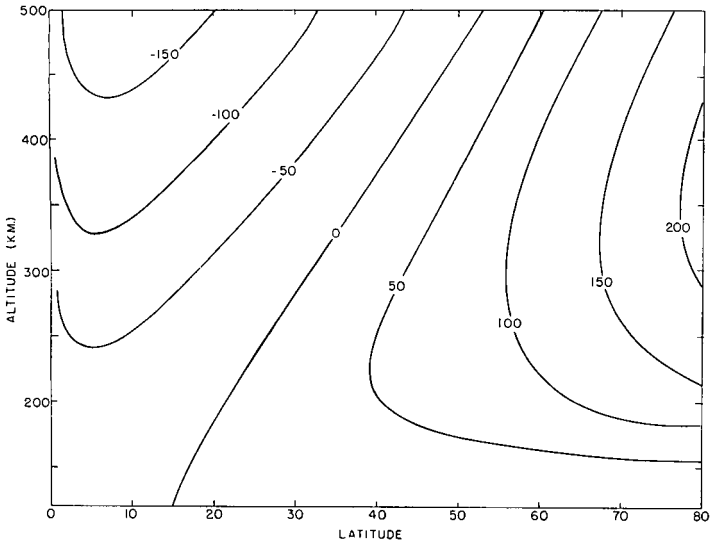

FIGURE 13.—The zonally averaged pressure gradient force obtained from the temperature field of the previous figure. Units are 10^{-4} m. sec.$^{-2}$

altitude in Paper I leads to the conclusion that motion in the thermosphere is governed by the pressure gradient force below about 300 km., the atmosphere at higher levels being dragged around by the action of viscosity. The zonally averaged pressure gradient force in figure 13 would then be expected to give rise to a substantial mean meridional motion directed toward the Pole in middle and high latitudes and a relatively small equatorward drift in low latitudes. Any correlation between deviation of ion drag and meridional wind from their respective zonal averages will also contribute to the mean meridional cell, but this will not be examined here.

The modified meridional cell produced by the hypothetical decrease of the parameter s with latitude will give descent in polar regions and concomitant adiabatic heating. If the variation of s as assumed above is introduced into the JS model, the lower massive part of the thermosphere will behave as a *heat engine*, and the high densities seen at great heights in polar regions become explicable in terms of adiabatic heating in high latitudes.

When the JS model is modified by allowing s to decrease with latitude, a further correction is necessary to restore full agreement with the high latitude satellite drag densities. Comparison of figures 10 and 12 reveals that the assumed change in the temperature field introduces a cooler layer poleward of 30° and below about 250 km. A compensating warmer layer must be introduced above 250 km. if the variation of density with latitude at high levels is to remain unaltered by the decrease of s. The change in the zonally averaged exospheric temperature which hydrostatically compensates for the cooler temperatures introduced at lower levels can be calculated from equations (12) and (A.1) and the ideal gas law. Results of this calculation for the variation of s that has been assumed for the example discussed above are shown in table 2. The first row of the table contains values of the zonally averaged exospheric temperature for the unmodified JS model used in Paper I.

TABLE 2.—*Zonal average exospheric temperature and correction*

Latitude:	15	30	40	60	80
$\overline{T}_\infty$(°K.)	885	895	903	912	916
$\Delta\overline{T}_\infty$(°K.)	1	3	6	14	25

In the second row of the table is the increment that must be added if the zonally averaged density at 600 km. is to remain the same when s decreases with latitude according to equation (12) with $b=0.5$. A corrected global pattern of exospheric temperature for the modified model is then given by adding this increment, which is independent of local time, to the pattern of isotherms in figure 1. This correction introduces a small correction in the temperature field at lower levels. A correct fit to the zonally averaged density at 600 km. would be obtained by further iteration.

5. SUMMARY AND CONCLUSIONS

Values of horizontal winds obtained by Geisler [4] have been used to deduce the global field of vertical motion in the thermosphere. The vertical motions are of the order of 1 m. sec.$^{-1}$ and give adiabatic heating and cooling which is comparable to the heating by solar radiation. This result supports the conclusion (Dickinson, Lagos, and Newell [2]; Lagos [11]) that the distribution of adiabatic heating and cooling by vertical motion will influence the shape and phase of the diurnal bulge.

In order to analyze the factors which govern the distribution of the adiabatic sources and sinks of heat, the vertical motion was decomposed into separate parts. As discussed in section 3, the vertical motion arising from the divergence of the zonal wind has the correct phase to advance the phase of the diurnal bulge in local time. This tendency is reinforced in low latitudes by the vertical motion arising from divergence of the time-varying part of the meridional wind. The zonally averaged (or time-averaged) meridional wind produces a meridional circulation which gives adiabatic cooling in middle and high latitudes, a result which is considered unrealistic.

The deduced meridional circulation is interpreted to be a consequence of the fact that the zonally averaged temperature increases poleward at all levels in the thermospheric temperature model used to calculate horizonal winds. A modification of the temperature model to give a mean poleward decrease of temperature at low levels was suggested. A numerical example was carried out to show that the zonally averaged pressure gradient is reversed in the modified model. This would drive a meridional circulation opposite to that derived from the winds of Paper I, providing subsidence and adiabatic heating in high latitudes.

The present paper and Paper I indicate that dynamical calculations can be useful in the formulation of empirical models of the thermosphere. The discussion of the present paper suggests a way in which a particular empirical model can be modified. To arrive at a thermodynamically consistent temperature model an iterative procedure is required, combining full calculation of the motion field

with each modification, until there is not only agreement with the density data but also a proper balance between the various thermospheric heat sources.

APPENDIX

DEPENDENCE OF PRESSURE GRADIENTS ON THE PARAMETERS T_∞ AND s

The intent of the following analysis is to obtain an analytic expression which describes approximately the dependence of pressure gradient force upon the exospheric temperature T_∞ and the parameter s. We make use of the hydrostatic equation (6) and the ideal gas law in the form $p=\rho RT$, where R is the mean gas constant averaged over the various constituents. We shall assume that R and the acceleration of gravity g are constants. These assumptions are not crucial to the quantitative results which follow and are made only to simplify the analytic treatment. With these assumptions, the hydrostatic equation (6) integrates to

$$p=p_0 \exp\left[-gZ/RT_\infty\right] \tag{A.1}$$

where p_0 is the pressure at the lower boundary at 120 km. The quantity Z can be considered an *effective height* which is given by

$$Z=\int_0^z (T_\infty/T)\,dz=z+s^{-1}\log\left(T/T_0\right) \tag{A.2}$$

where use has been made of equation (1) in evaluating the integral and z is altitude above the lower boundary.

The pressure gradient force is $-\rho^{-1}\nabla_H p$, where ∇_H denotes the horizontal gradient operator. Differentiation of equation (A.1) with substitution from equations (1) and (A.2) gives an expression which can be put into the form

$$\frac{1}{\rho}\nabla_H p=g\left(\frac{T}{T_\infty}\right)\left[A\,\nabla_H(\log T_\infty)+B\,\nabla_H(\log s)\right], \tag{A.3}$$

where

$$A=z-s^{-1}\left[\left(\frac{T_\infty}{T}\right)\left(\frac{T-T_0}{T_\infty-T_0}\right)-\log\left(\frac{T}{T_0}\right)\right]$$

$$B=s^{-1}\log\left(\frac{T}{T_0}\right)-z\left(\frac{T_\infty}{T_0}-1\right).$$

The term in brackets in the definition of A is nearly constant above about 200 km. Hence, when s is assumed to be independent of the horizontal spatial variables, we recover the empirical result of Geisler [3] that the pressure gradient force is closely approximated by the product of a factor linear in z and the gradient of T_∞. It may be shown that B is always positive with positive s, while A is positive above 125 km. for the parameters of Paper I. Since the zonally averaged T_∞ increases with latitude in the JS model, the parameter s must be chosen to decrease with latitude in order to reverse the sign of the zonally averaged pressure gradient.

ACKNOWLEDGMENTS

This study has been supported by funds supplied by the National Science Foundation (grant No. GA-400) and by the Atomic Energy Commission (contract No. AT(30-1)2241).

REFERENCES

1. D. R. Bates, "Some Problems Concerning the Terrestrial Atmosphere Above the 100 Km. Level," *Proceedings of the Royal Society of London*, Ser. A, Vol. 253, No. 1275, Dec. 1959, pp. 451–462.
2. R. E. Dickinson, C. P. Lagos, and R. E. Newell, "Dynamics of the Neutral Gas in the Thermosphere for Small Rossby Number Motions," *Journal of Geophysical Research*, Vol. 73, No. 13, July 1968, pp. 4299–4313.
3. J. E. Geisler, "Atmospheric Winds in the Middle Latitude F-Region," *Journal of Atmospheric and Terrestrial Physics*, Vol. 28, No. 8, Aug. 1966, pp. 703–720.
4. J. E. Geisler, "A Numerical Study of the Wind System in the Middle Thermosphere," *Journal of Atmospheric and Terrestrial Physics*, Vol. 29, No. 12, Dec. 1967, pp. 1469–1482.
5. I. Harris and W. Priester, "Time-Dependent Structure of the Upper Atmosphere," *Journal of the Atmospheric Sciences*, Vol. 19, No. 4, July 1962, pp. 286–301.
6. S. L. Hess, *Introduction to Theoretical Meteorology*, Henry Holt and Co., New York, 1959, 362 pp.
7. L. G. Jacchia, "Static Diffusion Models of the Upper Atmosphere With Empirical Temperature Profiles," *Smithsonian Contributions to Astrophysics*, Washington, D.C., Vol. 8, 1965, pp. 215–257.
8. L. G. Jacchia and J. Slowey, "The Shape and Location of the Diurnal Bulge in the Upper Atmosphere," *Space Research 7*, North-Holland, R. L. Smith-Rose, Vol. 2, 1967, pp. 1077–1090.
9. D. G. King-Hele and R. R. Allan, "The Rotational Speed of the Upper Atmosphere," *Space Science Reviews*, Dordrecht, Holland, Vol. 6, No. 2, Nov. 1966, pp. 248–275.
10. H. Kohl and J. W. King, "Atmospheric Winds Between 100 and 700 Km. and Their Effects on the Ionosphere," *Journal of Atmospheric and Terrestrial Physics*, Vol. 29, No. 9, Sept. 1967, pp. 1045–1062.
11. C. P. Lagos, "On the Dynamics of the Thermosphere," *Planetary Circulations Project Report* No. 20, M.I.T. Department of Meteorology, 1967, 134 pp.
12. C. P. Lagos and J. R. Mahoney, "Numerical Studies of Seasonal and Latitudinal Variability in a Model Thermosphere," *Journal of the Atmospheric Sciences*, Vol. 24, No. 1, Jan. 1967, pp. 88–94.
13. R. S. Lindzen, "Reconsideration of Diurnal Velocity Oscillation in the Thermosphere," *Journal of Geophysical Research*, Vol. 72, No. 5, Mar. 1967, pp. 1591–1985.
14. R. E. Newell, "Thermospheric Energetics and a Possible Explanation of Some Observations of Geomagnetic Disturbances and Radio Aurorae," *Nature*, London, Vol. 211, No. 5050, Aug. 1966, pp. 700–703.

[*Received January 15, 1968; revised March 15, 1968*]